# Muon capture reaction on $^{100}$Mo to study the nuclear response for double-$\beta$ decay and neutrinos of astrophysics origin

I. H. Hashim*
*Physics Department, Faculty of Science, Universiti Teknologi Malaysia, 81310 Johor Bahru, Malaysia; Department of Physics, Osaka University, 560-0043 Toyonaka-shi, Osaka, Japan; and Research Center for Nuclear Physics, Osaka University, 567-0047 Ibaraki-shi, Osaka, Japan*

H. Ejiri,† T. Shima, and K. Takahisa
*Research Center for Nuclear Physics, Osaka University, 567-0047 Ibaraki-shi, Osaka, Japan*

A. Sato and Y. Kuno
*Department of Physics, Osaka University, 560-0043 Toyonaka-shi, Osaka, Japan*

K. Ninomiya
*Department of Chemistry, Osaka University, 560-0043 Toyonaka-shi, Osaka, Japan*

N. Kawamura and Y. Miyake
*Muon Science Laboratory, Institute of Materials Structure Science, High Energy Accelerator Research Organization (KEK), Tsukuba, Ibaraki 305-0801, Japan and Muon Science Section, Materials and Life Science Division, Japan Proton Accelerator Research Complex (J-PARC), Tokai, Ibaraki 319-1195, Japan*

(Received 30 July 2017; revised manuscript received 7 November 2017; published 30 January 2018)

Ordinary muon capture (OMC) on enriched $^{100}$Mo isotopes was studied for the first time to investigate neutrino nuclear responses for neutrinoless double-$\beta$ decays and supernova neutrino nuclear interactions. Muon capture on $^{100}$Mo proceeds mainly as $^{100}$Mo$(\mu,xn)^{100-x}$Nb with $x$ being the number of neutrons emitted from negative muon capture. The Nb isotope mass distribution was obtained by measuring delayed $\gamma$ rays from radioactive $^{100-x}$Nb. By using the neutron emission model after the muon capture, the neutrino response (the strength distribution) for OMC was derived. The OMC strength distribution shows a giant resonance (GR) at the peak energy around 11–14 MeV, suggesting the concentration of the OMC strength at the muon GR region.

DOI: 10.1103/PhysRevC.97.014617

## I. INTRODUCTION

Neutrino nuclear responses are crucial for neutrino studies in nuclei. Neutrino properties such as the Majorana nature, the absolute mass scale, and others beyond the standard electroweak model are studied by investigating neutrinoless double-$\beta$ decays ($0\nu\beta\beta$) as discussed in recent review papers [1–4] and references therein. Here the $\nu$ responses for $0\nu\beta\beta$ ($\beta^-$ and $\beta^+$ responses) are necessary to study the neutrino properties beyond the standard model. The $0\nu\beta\beta$ matrix element is associated with the $\beta^-$ and $\beta^+$ matrix elements of $M(\beta^-)$ and $M(\beta^+)$. Astroneutrino nucleosyntheses and astroneutrino nuclear reactions are studied by investigating astroneutrino nuclear interactions. Then one needs nuclear responses for astroneutrinos and astroantineutrinos [5]. So far, the single-$\beta^-$ matrix element $M(\beta^-)$ and the astroneutrino response have been extensively studied by nuclear charge exchange reactions as discussed in review papers [1,2,5] and references therein.

The present paper aims to show that ordinary muon capture (OMC) used to study the neutrino nuclear responses is relevant to the $\beta^+$ response associated with $0\nu\beta\beta$ and antineutrino response involved in astroantineutrino reactions. The OMC response for $^{100}$Mo shows a giant resonance (GR) distribution at the concentrated peak energy around 11–14 MeV.

OMC is a kind of muon charge exchange reaction via the weak boson W$^{\pm}$, where a negative muon becomes a muon neutrino and a proton in the target nucleus transforms into a neutron. The OMC response is given by the square of the nuclear matrix element $M(\mu)$. The reaction and the nuclear matrix element (NME) are expressed as

$$\mu + {}^{A}_{Z}X \rightarrow {}^{A}_{Z-1}Y + \nu_{\mu}, \ M(\mu), \tag{1}$$

where ${}^{A}_{Z}X$ with $A$ and $Z$ being the mass number and the atomic number of the target nucleus and ${}^{A}_{Z-1}Y$ is the remaining nucleus after OMC. The corresponding astroantineutrino reaction and

*izyan@utm.my
†ejiri@pop07.odn.ne.jp

 

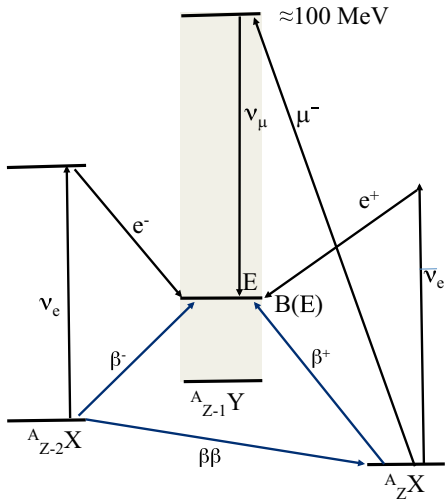


FIG. 1. Reaction and decay schemes for neutrinos, astroantineutrinos and double-$\beta$ decays.

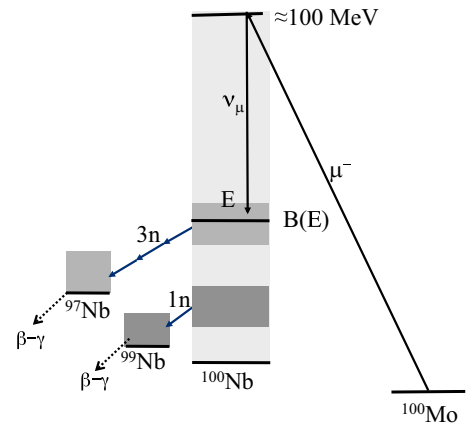


FIG. 2. Reactions and decay schemes for OMC on $^{100}$Mo. Highly excited states in $^{100}$Nb around 30 MeV deexcites by emitting three neutrons, populating finally the $^{97}$Nb RI, while those around 12 MeV deexcite by emitting one neutron, populating finally the $^{99}$Nb. The residual nuclei are identified by observing $\gamma$ rays characteristic of the RIs.

the NME are given as

$$\bar{\nu}_e + {}^{A}_{Z}X \rightarrow {}^{A}_{Z-1}Y + e^+, \ M(\bar{\nu}). \tag{2}$$

The $0\nu\beta\beta$ via the light Majorana $\nu$ exchange process with the $\beta^+$ and $\beta^-$ responses is written as the neutrino emission and reabsorption by,

$$ {}^{A}_{Z}X \rightarrow {}^{A}_{Z-1}Y + \nu_e + e^+, \ M(\beta^+). \tag{3}$$

$$ {}^{A}_{Z-2}X \rightarrow {}^{A}_{Z-1}Y + \bar{\nu}_e + e^-, \ M(\beta^-), \tag{4}$$

where $^{A}_{Z-1}Y$ is the intermediate nucleus. Note that the $\mu, \bar{\nu}$, and $\beta^+$ NMEs are associated with $\tau^+ \ p \rightarrow n$ transition, while $\nu$ and $\beta^-$ NMEs are with $\tau^- \ n \rightarrow p$ transition.

These reactions and decay schemes are shown in Fig. 1. Here the $0\nu\beta\beta$ NME $M_i(\beta\beta)$ is given by the sum of NMEs $M_i(\beta)$ over all relevant states in the intermediate nucleus $^{A}_{Z-1}Y$. The NMEs $M_i(\beta\beta)$ are associated indirectly with the single-$\beta$ NMEs of $M_i(\beta^+)$ and $M_i(\beta^-)$ via the intermediate state $i$. Thus information of $M_i(\beta^\pm)$ is used to help evaluate $M_i(\beta\beta)$.

Theoretical calculations of NMEs for neutrino nuclear responses are challenging since they are very sensitive to nuclear correlations, nuclear medium effects, and nuclear models, as discussed in review articles [1,2,6,7] and references therein. Thus experimental studies of them are very valuable. Experimental studies of the neutrino nuclear responses for $0\nu\beta\beta$ and astroneutrinos are described in review articles [1,2,5,8] and references therein.

The NMEs $M(\nu)$ for astroneutrino and the $M(\beta^-)$ for $0\nu\beta\beta$ (the left-hand side of Fig. 1) have been studied extensively by using high-energy-resolution ($^3$He,t) experiments at RCNP [1,2,5]. The reactions are nuclear charge exchange reactions via charged meson. On the other hand, there are no appropriate high-energy-resolution nuclear probes for the astroantineutrino $M(\bar{\nu})$ and $0\nu\beta\beta$ $M(\beta^+)$ (the right-hand side of Fig. 1).

The present OMC provides useful information relevant to $M(\bar{\nu})$ and $M(\beta^+)$ (the left-hand side of Fig. 1). Unique features of OMC is the large mass energy ($E$ = 0–50 MeV) and momentum $p$ = 20–100 MeV/c regions, which are the regions involved for $0\nu\beta\beta$ and medium-energy supernova antineutrinos.

In OMC, a well-bound proton in the target nucleus $^{A}_{Z}X$ is shifted up to a vacant neutron shell, and one gets mostly the excited nucleus $^{A}_{Z-1}Y^*$ with the excitation energy $E$. If it is particle bound, it decays by emitting $\gamma$ rays to the ground state of $^{A}_{Z-1}Y$. On the other hand, if $^{A}_{Z-1}Y^*$ is unbound, it deexcites by emitting a number ($x$) of neutrons in case of medium-heavy nucleus since proton emission is suppressed much by the Coulomb barrier.

Finally, one residual nucleus $^{A-x}_{Z-1}Y$ is obtained. If it is radioactive, we may identify it by measuring characteristic $\gamma$ rays of the residual nucleus. The number of the emitted neutrons reflects the excitation energy $E$, larger $x$ corresponds to the higher $E$ region. Thus one can derive the OMC response (the strength distribution) as a function of $E$, from the mass $(A - x)$ distribution of the residual isotopes, as suggested in 1972 [9], and also in more recent years [10–12]. The OMC and the neutron emission schemes are illustrated in Fig. 2.

So far nuclear $\gamma$ rays from OMC were measured to study the nuclear reaction mechanisms [13–15]. Prompt $\gamma$ rays from bound states excited by muon capture $^{A}_{Z}X(\mu, xn\gamma)^{A-x}_{Z-1}Y$ reactions were investigated to study $\beta^+$ responses for low-lying bound states [16]. The OMC reactions to such low-lying spin states provide useful information on nuclear matrix elements for intermediate states in $0\nu\beta\beta$ and two-neutrino double-$\beta$ decays ($2\nu\beta\beta$).

Theoretical studies on the OMC cross sections for low-lying states in double-$\beta$ decay nuclei were made in terms of the pn-QRPA [17–20]. Experimental studies were tried on several double-$\beta$ decay nuclei [16,21,22]. Here it is hard to extract the $\beta^+$ strengths to individual states because the states are populated not only directly by OMC but also indirectly via $\gamma$ transitions from higher states populated by OMC via $\gamma$ transitions.

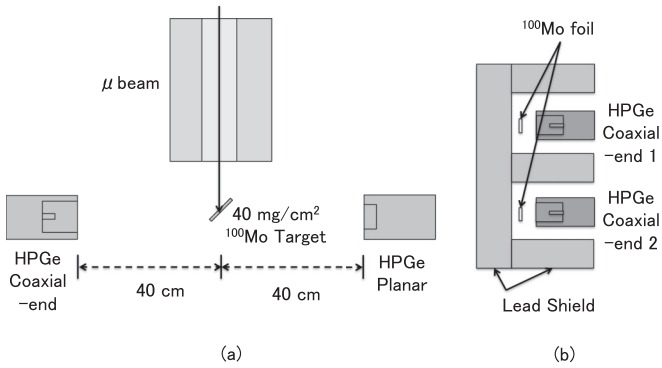


FIG. 3. Schematic plane view of (a) the target and the coaxial-type Ge detectors for prompt X and prompt/short-lived $\gamma$-rays and (b) the Ge detectors for the off-line measurements for the long-lived RIs.

In the present work, we focus on the gross structure of the OMC strength distribution over the wide excitation region of $E = 0$–$60$ MeV by measuring the residual isotopes (RIs) ${}^{A-x}Y$. The RI yield is well obtained by measuring the yield of $\gamma$ rays from ${}^{A-x}Y$ and the known $\gamma$-branching ratio. A neutron emission code was developed to link the mass number $A - x$ of the residual nucleus to the initial excitation energy $E$ of ${}^{A}_{Z-1}Y^{*}$ [23].

## II. MUON IRRADIATION EXPERIMENT

The present OMC experiment is made on ${}^{100}_{42}$Mo as a typical medium heavy nucleus for astrophysics and $0\nu\beta\beta$ interests [24,25]. The target used is a thick $^{100}$Mo with 40 mg/cm$^2$. Low-energy $\mu^-$ beams with $p = 28$ MeV/c from the D-beam line at J-PARC Material Life Science Facility (MLF) were used to irradiate the target for seven hours. Here most muons were stopped and captured into the target nucleus to form excited states in ${}^{100}_{41}$Nb. Then $\gamma$ rays from short-lived Nb isotopes with $A = 100$ and 99 were measured on-line using planar and coaxial-end-type HPGe detectors as shown in the left-hand side of Fig. 3, while $\gamma$ rays from long-lived Nb isotopes and other isomers were measured off-line in a separate room by using two coaxial Ge detectors as shown in the right-hand side of Fig. 3.

## III. $\gamma$ RAYS FROM OMC ON ENRICHED MO AND NB MASS DISTRIBUTION

The prominent $\gamma$-ray peaks from short-lived and long-lived Nb isotopes were clearly observed as shown in Fig. 4. The typical $\gamma$ rays from the OMC products are listed in Table I. The 535.0 keV $\gamma$ ray from the short-lived $^{100}$Nb and 137 keV $\gamma$ ray from the short-lived $^{99}$Nb were measured by the online Ge detector setup, while others from the long-lived $^{99}$Mo, $^{99m}$Tc, $^{98}$Nb, $^{97}$Nb, $^{96}$Nb, and $^{95}$Nb were measured by the off-line Ge detector setup. Among them, the 66 h $^{99}$Mo is the $\beta^-$-decay product from $^{99}$Nb and the 6 h $^{99m}$Tc is the isomeric state produced by the $\beta^-$ decay from $^{99}$Nb.

The number of the Nb RIs ${}^{100-x}$Nb produced by OMC on $^{100}$Mo was evaluated from the observed $\gamma$-ray yields corrected for the Ge detector efficiency, the $\gamma$-ray branching ratio,

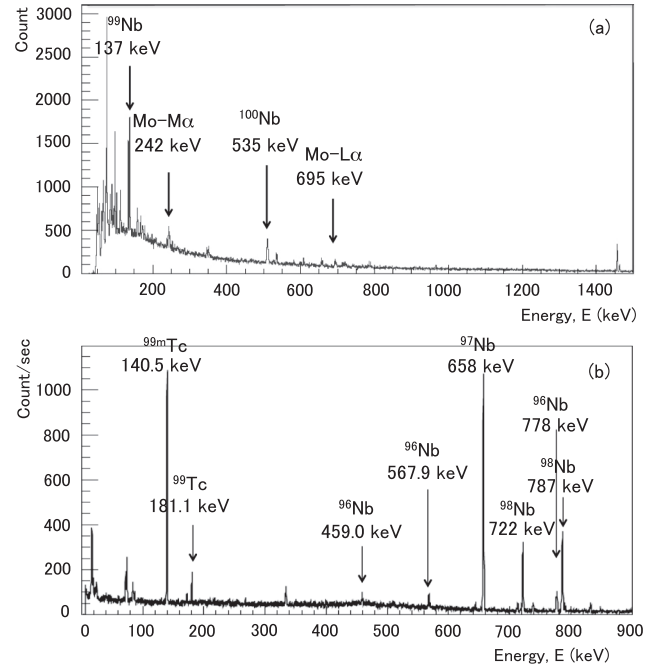


FIG. 4. $\gamma$-ray spectra from OMC on $^{100}$Mo. (a) Online spectrum for the prompt $\gamma$ rays and delayed ones from short-lived RIs. (b) Off-line spectrum for the delayed $\gamma$ rays from long-lived RIs. The 242 keV and 695 keV line in (a) is the muonic x ray. Note the x-ray yields are much reduced due to the pile up effect.

and their decays during the muon irradiation and the $\gamma$-ray measurement. The obtained RI mass $(A - x)$ distribution is shown in Fig. 5. The $^{100}$Nb yield at $x = 0$ is small, but the ${}^{100-x}$Nb yield jumps up drastically at $x = 1$, and decreases gradually as $x$ increases down to the mass $A = 95$ and $x = 5$. This is similar to the distributions in other target nuclei [11,13–15].

Let us evaluate the RI mass distribution on the basis of the OMC strength distribution and the statistical neutron emission model [26]. The OMC excitations are expressed in terms of the vector excitations with the spin transfers of $\Delta J^\pi = 0^+, 1^-, 2^+$ and the axial-vector ones with $\Delta J^\pi = 1^+, 2^-$. Pseudoscalar contributions are also involved. Among them, the $0^+$ Fermi

TABLE I. Nuclear isotopes observed by OMC $(\mu, xn)$ reactions. Half-lives are given by s (second), min (minute), h (hour), or d (day).

| Isotope | lifetime | Energy(keV) |
|---|---|---|
| $^{100}$Nb | 2.99 s | 535.0 |
| $^{99}$Nb | 2.6 min | 137.0 |
| $^{99}$Mo | 66.0 h | 181.1, 739.5 |
| $^{99m}$Tc | 6 h | 140.5 |
| $^{98}$Nb | 1.23 h | 722.0, 787.0 |
| $^{97}$Nb | 0.85 h | 657.9 |
| $^{96}$Nb | 23.3 h | 459.0, 568.7, 778.0 |
| $^{95}$Nb | 34.9 d | 765.0 |
| $^{94}$Nb | 51.8 min | 75.5, 366.9, 891.7 |
| $^{93}$Nb | 6.85 h | 2424.9 |

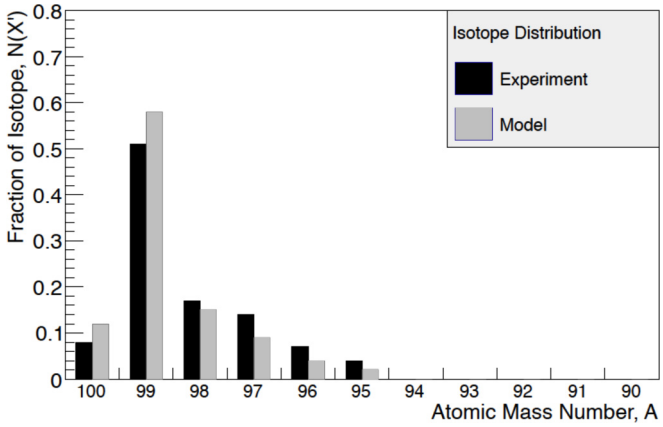


FIG. 5. Nb RI mass distribution for OMCs on $^{100}$Mo. The black and light gray histograms are the experimental and calculated yields.

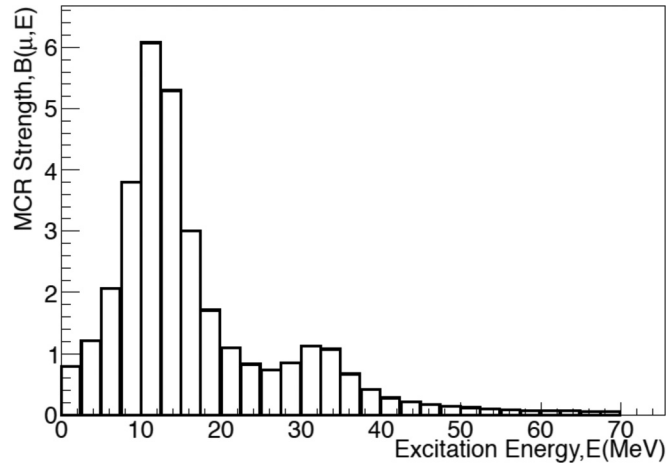


FIG. 6. The OMC strength distribution suggested from the experimental RI distribution. $E_{G1}$ and $E_{G2}$ are the OMC GRs at around 12 MeV and 30 MeV.

and the $1^+$ Gamow-Teller (GT) excitations are reduced much since the $0\hbar\omega$ Fermi and GT excitations for the $\beta^+$ and the antineutrino responses are blocked by the neutron excess in medium-heavy nuclei of the present interest. The $1^-$ excitation with the $1\hbar\omega$ transition may show the giant resonance (GR) like the electric dipole ($E1$) GR in case of the photon capture reaction (PCR).

The vector $2^+$ and the axial-vector $2^-$ excitations may show broad GR-like distributions as the $2\hbar\omega$ and spin-dipole GRs. Accordingly, we assume OMC strength distribution of $B(\mu,E)$ given by the sum of the two GR strengths of $B_1(\mu,E)$ and $B_2(\mu,E)$,

$$B(\mu,E) = B_1(\mu,E) + B_2(\mu,E), \tag{5}$$

$$B_i(\mu,E) = \frac{B_i(\mu)}{(E - E_{Gi})^2 + (\Gamma_i/2)^2}, \tag{6}$$

where $E_{Gi}$ and $\Gamma_i$ with $i = 1$ and 2 are the GR energy and the width for the $i$th GR, and the constant $B_i(\mu)$ is expressed as $B_i(\mu) = \sigma_i\Gamma_i/(2\pi)$ with $\sigma_i$ being the total strength integrated over the excitation energy.

Excited states ${}^{A}_{Z-1}Y^*$ populated by OMC deexcite mostly by emitting neutrons at the preequilibrium (PEQ) and equilibrium (EQ) stages [23,26,27]. If they are neutron unbound, and they decay by emitting $\gamma$ rays to the ground state if they are bound. Here we ignore proton emission, which is prohibited by the Coulomb barrier in case of the medium and heavy nuclei. The energy spectrum of the first neutron $E^1_n$ is given by [26].

$$S(E^1_n) = k\left[E^1_n exp\left(-\frac{E^1_n}{T_{\rm EQ}(E)}\right) + pE^1_n exp\left(-\frac{E^1_n}{T_{\rm PEQ}(E)}\right)\right], \tag{7}$$

where $E^1_n$ is the first neutron kinetic energy, $T_{\rm EQ}(E)$ and $T_{\rm PEQ}(E)$ are the EQ and PEQ nuclear temperatures and $p$ is the fraction of the PEQ neutron emission. The neutron emission from the EQ stage is a kind of neutron evaporation from thermal equilibrium phase.

The EQ temperature is expressed as $T_{\rm EQ}(E) = \sqrt{(E/a)}$ with $a$ being the level density parameter [26]. The parameter $a$ is expressed as $a = A/8$ MeV for the nucleus with mass number $A$. $T_{\rm PEQ}(E)$ is given by $b \times T_{\rm EQ}(E)$ with $b \approx 3$ for OMC with low-momentum (≈50–90 MeV/c) and low-excitation ($E \approx$ 10–50 MeV). The PEQ contribution for the first neutron emission depends on the nuclear size, getting smaller as the nuclear size becomes larger. It is estimated to be around $p \approx 0.6A^{-1/3}$ for the present OMC case by referring to the observed neutron energy spectra [11,28,29].

The residual nucleus ${}^{A-1}_{Z-1}Y$ after the first neutron emission deexcites by emitting the second neutron or $\gamma$ rays depending on the excitation energy above or below the neutron threshold energy. The ground state of ${}^{A-1}_{Z-1}Y$ is populated after the $\gamma$ emission. The second neutron $n_2$ is the EQ evaporation neutron, and then the third neutron is emitted if the residual nucleus after the second neutron emission is neutron unbound, and so on. Then, one gets finally the residual isotopes of ${}^{A-x}_{Z-1}Y$ with $x = 0,1,2,3,\ldots$ depending on the excitation energy $E$ and the number $x$ of the emitted neutrons. They are $\beta$-unstable RIs. The neutron number $x$ and the mass number $A - x$ distributions reflect the strength distribution $B(\mu,E)$ of the nucleus ${}^{A}_{Z-1}Y^*$ after OMC, the highly excited states around 30–40 MeV emit 3–4 neutrons while the low excited states around 11–14 MeV emit one neutron as illustrated in Fig. 6. In other words, the GR-like strength around 11–14 MeV leads preferentially to the population of ${}^{A-1}_{Z-1}Y$ after 1 neutron emission, and the population of ${}^{A-x}_{Z-1}$y decreases as $x$ increases. These features have been observed previously in Refs. [11,12,16,23].

We compare the observed RI mass distribution for OMC on $^{100}$Mo with the calculation based on the strength distribution and the EQ/PEQ neutron emission model. The obtained RI mass distribution is compared with the observed one in Fig. 6. The agreement with the observed data is quite good where $\chi^2$ is 0.06. The parameters used for the calculation are $E_{G1} =$ 12 MeV with $\Gamma_1 = 8$ MeV, $E_{G2} = 30$ MeV with $\Gamma_2 = 8$ MeV, and the cross-section ratio is $\sigma_1/\sigma_2 = 1/6$. The first GR corresponds to the large population of the mass $A - 1$ with $x = 1$ neutron emission, while the second GR reflects the population of the RIs with the mass around $A - 3$ and $A - 4$ with $x =$ 3–4 neutron emission.

The OMC GR may be compared with the photon capture reaction giant resonance (PCR GR). The energy of 12 MeV is smaller than the PCR GR energy of 14 MeV, but the width of 8 MeV is much larger than the width for PCR GR (5 MeV). The OMC GR consists of mixed components of $J^\pi = 1^-, 1^+, 2^-$ while PCR GR consists of only one component $J^\pi = 1^-$.

OMCs in other nuclei have been studied also as discussed in Refs. [11,13–15]. The one neutron emission is dominant in most OMCs, being consistent with the present observation on $^{100}$Mo, and with the GR strength corresponding to the one-neutron emission. Neutron energy spectra were observed for OMCs on $^{32}$S, $^{40}$Ca, $^{207}$Pb, and $^{209}$Bi. They reported low-energy EQ and medium-energy PEQ components from neutron time-of-flight (TOF) measurement. They are reproduced by the EQ/PEQ neutron emission model with the strength distribution given in Eq. (5). Recently, OMC strength distributions are evaluated theoretically by means of QRPA calculations [30].

## IV. SUMMARY

OMC is a lepton-sector charge exchange reaction via the weak boson, is shown to be used to study neutrino nuclear responses relevant to $0\nu\beta\beta$ and astroneutrino reactions. It provides unique information on $\beta^+$ side of $0\nu\beta\beta$ NMEs and astroantineutrino NMEs in the energy and momentum regions of $E \approx 0$–$50$ MeV and $p \approx 95$–$50$ MeV/c.

These are the regions associated with the $0\nu\beta\beta$ and supernova neutrinos. The Nb RIs produced by OMC on $^{100}$Mo are identified by measuring delayed $\gamma$ rays characteristic of the RIs. The Nb mass distribution shows a large yield at $A = 99$ after one ($x = 1$) neutron emission and decreases gradually as $A$ decreases to $A = 95$ ($x = 5$). The neutron emission is analyzed in terms of the EQ/PEQ neutron emission model. The observed RI distribution reflects the OMC strength distribution with a broad peak at $E \approx 11$–$14$ MeV and the small bump at $E \approx 30$–$40$ MeV. The broad peak is a kind of muon capture GR analogous to the $E1$ photon-capture GR. It is noted that similar GRs are observed for the $0\nu\beta\beta$ $\beta^-$-side responses and the astroneutrino responses [1,2,5]. The shift of the $\beta^+$ strength to the high-excitation GR suggests the strong spin isospin correlation, which may affect the $\beta^+$ side of $0\nu\beta\beta$ response.

## V. REMARKS AND PERSPECTIVES

The RCNP MuSIC DC muon beam and the J-PARC MLF pulsed muon beam are promising for further studies of neutrino nuclear responses. The lifetime measurement is in progress to study the absolute strength (square of absolute NME). The absolute response, together with the strength distribution, help theories to evaluate the $0\nu\beta\beta$ NMEs and astro-neutrino synthesis/interaction NMEs. In other words, nuclear models to be used for $0\nu\beta\beta$ NME calculations should reproduce the OMC strength distribution as observed. Experimental studies of OMCs on all $0\nu\beta\beta$ nuclei are under progress at RCNP[27].

The EQ/PEQ neutron emission code was developed for the neutron emission following OMC on the present $^{100}$Mo with the large neutron excess and $Z = 42$. One has to include proton emissions as well in medium heavy nuclei with less neutron excess since the proton binding energy becomes lower relative to the neutron binding energy, and also in light nuclei where the Coulomb barrier gets lower. The EQ/PEQ code with both neutrons and protons are being developed at UTM and RCNP.

The present experiment is made on delayed $\gamma$ rays from RIs produced by OMC to get the yields of the RIs since the $\gamma$-ray branching ratios are well known. Then we get the gross structure of the strength distribution up to $E \approx 60$ MeV. The strengths (responses) to individual states below the neutron threshold energy can be studied by measuring prompt $\gamma$-rays from OMC. OMC relative strength distributions and absolute OMC rate measurements for other double-$\beta$ decay nuclei are under progress to get OMC nuclear matrix elements to provide useful information for $0\nu\beta\beta$ matrix elements.

The population of the $i$th state is in principle obtained from the difference between the summed yield of all the $\gamma$ rays from the $i$th state and that of all the $\gamma$ rays feeding the $i$th state from higher states. However, in medium heavy nuclei with rather a high-level density, it is a challenge to measure accurately all the $\gamma$ rays from and to the individual states.

Exclusive programs for OMC $\gamma$ spectroscopy by using the CAGRA $\gamma$ detector array are under progress at RCNP.

We note that the present OMC strength distribution is used to evaluate the OMC RI production and RI transmutation rate, as presented elsewhere.

## ACKNOWLEDGMENTS

This project is funded through Fundamental Research Grant Scheme (FRGS) Grant No. R.J130000.7826.4F971 of the Ministry of Education Malaysia and Universiti Teknologi Malaysia. This work of Y.K. was supported in part by the Japan Society of the Promotion of Science (JSPS) KAKENHI Grant No. 25000004. The authors thank the Department of Physics, Graduate School of Science, Osaka University and RCNP Osaka University and MuSIC colleagues there for supporting the present experiments. We are grateful to Prof. H. Kosmas and Prof. J. Suhonen for valuable discussions. They are indebted to Yamada Science Foundation for the Neutrino Dark Matter (NDM03) Yamada Symposium and Muon X-ray Gamma (MXG16) Yamada workshop, where the present UTM and RCNP collaboration works were promoted.

[1] H. Ejiri, J. Phys. Soc. Jpn. **74**, 2101 (2005).
[2] J. Vergados, H. Ejiri, and F. Simkovic, Rep. Prog. Phys. **75**, 106301 (2012).
[3] F. Avignone, S. Elliott, and J. Engel, J. Rev. Mod. Phys. **80**, 481 (2008).
[4] J. Vergados, H. Ejiri, and F. Simkovic, Int. J. Mod. Phys. E **25**, 1630007 (2016).
[5] H. Ejiri, Phys. Rep. C **338**, 265 (2000), and references therein.
[6] J. Suhonen and O. Osvaldo, J. Phys. Rep. **300**, 123 (1998).
[7] A. Faessler and F. Simkovic, J. Phys. G **24**, 2139 (1998).
[8] J. Engel and J. Menendez, Rep. Prog. Phys. **80**, 046301 (2017).
[9] H. Ejiri, in *Proceedings of the International Conference on Electromagnetic Interactions, Sendai, 1972* (Tohoku University, Sendai, 1972).

[10] H. Ejiri, Czech. J. Phys. **56**, 459 (2006).
[11] D. F. Measday, Phys. Rep. **354**, 243 (2001).
[12] H. Ejiri, I. H. Hashim *et al.*, J. Phys. Soc. Jpn. **82**, 044202 (2013).
[13] H. J. Evans, Nucl. Phys. A **207**, 379 (1973).
[14] G. R. Lucas Jr., P. Martin, G. H. Miller, R. E. Welsh, D. A. Jenkins, R. J. Powers, and A. R. Kunselman, Phys. Rev. C **7**, 1678 (1973).
[15] R. Raphael, H. Überall, and C. Werntz, Phys. Lett. **24B**, 15 (1967).
[16] V. Egorov *et al.*, Czech. J. Phys. **56**, 453 (2006).
[17] M. Kortelainen and J. Suhonen, Europhys. Lett. **58**, 666 (2002).
[18] M. Kortelainen and J. Suhonen, Nucl. Phys. A **713**, 501 (2003).
[19] J. Suhonen, Czech. J. Phys. **56**, 511 (2006).
[20] J. Suhonen and M. Kortelainen, Int. J. Mod. Phys. E **17**, 1 (2008).
[21] D. Zinatulina, V. Brudanin, Ch. Briançon, V. Egorov, C. Petitjean, M. Shirchenko, R. Vasiliev, and I. Yyutlandov, AIP Conf. Proc. **1572**, 122 (2014).
[22] D. R. Zinatulina, Ch. Briançon, V. B. Brudanin, R. V. Vasilyev, K. Ya. Gromov, V. G. Egorov, C. Petitjean, V. I. Fominykh, V. G. Chumin, M. V. Shirchenko, and I. A. Yutlandov, Bul. Russ. Aca. Sci. Phys. **74**, 825 (2010).
[23] I. H. Hashim, Ph.D. thesis, Osaka University, 2014.
[24] H. Ejiri, J. Engel, R. Hazama, P. Krastev, N. Kudomi, and R. G. H. Robertson, Phys. Rev. Lett. **85**, 2917 (2000).
[25] H. Ejiri, J. Engel, and N. Kudomi, Phys. Lett. B **530**, 27 (2002).
[26] H. Ejiri and M. J. A. de Voigt, *Gamma-Ray and Electron Spectroscopy in Nuclear Physics* (Oxford University Press, Oxford, 1989).
[27] I. H. Hashim and H. Ejiri *et al.*, *Proposal for WSS-MuSIC beamtime* (Osaka University, Osaka, 2016).
[28] T. Kozlowski, A. Zglinski *et al.*, Nucl. Phys. A **436**, 717 (1985).
[29] N. C. Mukhopadhyay, Phys. Rep. **30**, 1 (1977).
[30] H. Kosmas and H. Ejiri (private communication).